Cathepsin S from both tumour and tumour-associated cells promote cancer growth and neovascularisation

Small, D. M., Burden, R. E., Jaworski, J., Hegarty, S. M., Spence, S., Burrows, J. F., McFarlane, C., Kissenpfennig, A., McCarthy, H. O., Johnston, J. A., Walker, B., & Scott, C. J. (2013). Cathepsin S from both tumour and tumour-associated cells promote cancer growth and neovascularisation. *International Journal of Cancer*, *133*(9), 2102-2112. https://doi.org/10.1002/ijc.28238

Published in:
International Journal of Cancer

Document Version:
Peer reviewed version

Queen's University Belfast - Research Portal:
Link to publication record in Queen's University Belfast Research Portal

Publisher rights
© 2013 UICC.
This work is made available online in accordance with the publisher's policies. Please refer to any applicable terms of use of the publisher.

General rights
Copyright for the publications made accessible via the Queen's University Belfast Research Portal is retained by the author(s) and / or other copyright owners and it is a condition of accessing these publications that users recognise and abide by the legal requirements associated with these rights.

Take down policy
The Research Portal is Queen's institutional repository that provides access to Queen's research output. Every effort has been made to ensure that content in the Research Portal does not infringe any person's rights, or applicable UK laws. If you discover content in the Research Portal that you believe breaches copyright or violates any law, please contact openaccess@qub.ac.uk.

Download date:08. May. 2023

Accepted Article

Title

Cathepsin S from both tumour and tumour-associated cells promote cancer growth and neovascularisation.

Authors

Donna M Small[1], Roberta E Burden[1], Jakub Jaworski[1], Shauna M Hegarty[2], Shaun Spence[3], James F Burrows[1], Cheryl McFarlane[3], Adrien Kissenpfennig[3], Helen O McCarthy[1], James A Johnston[2,4], Brian Walker[1] and Christopher J Scott[1*].

Affiliations

[1] School of Pharmacy, Queen's University Belfast, Lisburn Road, Belfast. BT9 7BL.

[2] School of Medicine, Dentistry and Biomedical Sciences, Queen's University Belfast, Lisburn Road, Belfast. BT9 7BL.

[3] Centre for Infection and Immunity, Health Sciences Building, Queen's University Belfast, Lisburn Road, Belfast. BT9 7BL.

[4] Inflammation Research, Amgen Inc, One Amgen Center Drive, Thousand Oaks, CA 91320, USA (present address).

*Corresponding author:

Christopher Scott

School of Pharmacy,

Queens University Belfast

This article has been accepted for publication and undergone full peer review but has not been through the copyediting, typesetting, pagination and proofreading process which may lead to differences between this version and the Version of Record. Please cite this article as an 'Accepted Article', doi: 10.1002/ijc.28238

97 Lisburn Road

Belfast UK

BT9 7BL

Email: c.scott@qub.ac.uk

Tel: +44(0)28 90 97 2350

Key words

Proteases, Cathepsin S, Angiogenesis, Tumourigenesis, Stroma.

Novelty and Impact

Cathepsin S is a protease that is upregulated in multiple tumour types. Using a syngeneic murine model, we were able to evaluate the contribution of cathepsin S from both tumour and tumour-associated cells, clearly showing for the first time that both sources can contribute this protease to promote tumourigenesis. These results reveal a mechanism by which tumour and recruited cells cooperate in tumour development and validate cathepsin S as an anti-angiogenic and anti-proliferative drug target.

Accepted Article

Accepted Article

Abstract

Recent murine studies have demonstrated that tumour-associated macrophages in the tumour microenvironment are a key source of the pro-tumourigenic cysteine protease, cathepsin S. We now show in a syngeneic colorectal carcinoma murine model that both tumour and tumour-associated cells contribute cathepsin S to promote neovascularisation and tumour growth. Cathepsin S depleted and control colorectal MC38 tumour cell lines were propagated in both wild type C57Bl/6 and cathepsin S null mice to provide stratified depletion of the protease from either the tumour, tumour-associated host cells, or both. Parallel analysis of these conditions showed that deletion of cathepsin S inhibited tumour growth and development, and revealed a clear contribution of both tumour and tumour-associated cell derived cathepsin S. The most significant impact on tumour development was obtained when the protease was depleted from both sources. Further characterisation revealed that the loss of cathepsin S led to impaired tumour vascularisation, which was complemented by a reduction in proliferation and increased apoptosis, consistent with reduced tumour growth. Analysis of cell types showed that in addition to the tumour cells, tumour-associated macrophages and endothelial cells can produce cathepsin S within the microenvironment. Taken together, these findings clearly highlight a manner by which tumour-associated cells can positively contribute to developing tumours and highlight cathepsin S as a therapeutic target in cancer.

Accepted Article

Introduction

Cathepsin S (CatS) is a cysteine protease, found abundantly in antigen presenting cells (APCs), where it is known to have key roles in MHC class II antigen processing and presentation.[1,2] This potent elastinolytic and collagenolytic enzyme is unique amongst the 11 human lysosomal cysteine cathepsins due to its ability to retain its activity in more neutral pH conditions, such as the extracellular environment.[3,4] Consequently, CatS has been implicated in a number of disease states, where it is secreted and promotes the remodelling of extracellular matrix (ECM) components, especially in conditions such as rheumatoid arthritis, atherosclerosis and cancer.[5-10]

Clinically, the up-regulation of CatS in tumours has been observed in prostate, gastric, colorectal and brain tumours.[11-14] Indeed, in astrocytomas, increased CatS levels correlate with advancing tumour grade and a poorer patient prognosis.[15,16] In addition, we have recently observed similar prognostic value in colorectal cancer (CRC), detecting marked up-regulation in all tumour stages.[13,17]

Further insight into the role(s) of CatS in tumour development has been provided using murine tumour models. CatS null ($CatS^{-/-}$) mice crossed with the spontaneous pancreatic beta cell carcinogenesis model (RIP1-Tag2) established that CatS can promote tumourigenesis through increased invasiveness, activation of angiogenesis and tumour neo-vascularisation.[10,18] It highlighted that a major source of CatS in these tumours was infiltrating tumour-associated macrophages (TAMs).[19] However, our previous analyses

Accepted Article

of human tumour cell lines and clinical biopsies from brain and colorectal carcinomas demonstrated that tumour cells also produce significant levels of this protease.[13-17,20] Therefore, in this current investigation, we wished to further evaluate the role and the cellular contribution of CatS in a syngeneic immuno-competent CRC tumour model, comparing both C57Bl/6 wild type (WT) and $CatS^{-/-}$ mice. These studies show a clear contribution of CatS from both tumour and tumour-associated cells, which promote angiogenesis and tumour progression, validating its potential as a therapeutic target.

Accepted Article

Materials and Methods

Cell lines

MC38 colon adenocarcinoma cells (S Rosenberg, NCI), B16-F10 murine melanoma cells (ATCC) and RAW 264.7 leukaemic monocyte macrophage cells (ATCC) were routinely cultured in DMEM (Invitrogen, UK) supplemented with 10% FBS (PAA, UK), 100 µg/ml penicillin and 100 µg/ml streptomycin (Invitrogen, UK). The Lewis lung carcinoma line (LLC) (ATCC) was similarly cultured in RPMI 1640 (Invitrogen, UK).

Immunofluorescent staining

Paraformaldehyde-fixed cells were stained overnight using goat anti-CatS or non-immune goat primary antibodies (R & D Systems, UK) (15 µg/ml) and secondary Alexa Fluor 488 rabbit anti-goat antibody (Molecular Probes, UK) (4 µg/ml, 30 min). Cells were rinsed and mounted with Vectashield with 4',6-diamidino-2-phenylindole (DAPI) (Vectorlabs, UK) counterstain, and visualized on the Leica TCS SP5 DMI6000 CS confocal microscope with Leica LAS AF software.

Reverse transcriptase-PCR

Detection and amplification of mRNA from STAT60 purified total RNA (Biogenesis, UK) for CatS and GAPDH was performed using the ImProm-II Reverse Transcriptase system (Promega, UK) following manufacturer's instructions. The following primers were used at an annealing temperature of 53 °C for 35 cycles: CatS (5' ATGAAACGGCTGGTTTGTGTGC '3, and 3'

Accepted Article

CTAGATTTCTGGGTAAGAGGG '5) and GAPDH (5' ACCACAGTCCATGCCATCAC '3 and 3'TCCACCACCCTGTTGCTGTA'5). The PCR products were visualized by agarose gel electrophoresis on a 1% gel.

Retroviral transfection and transductions

Murine CatS-specific short-hairpin RNAs (shRNA) and control constructs in pGFP-V-RS (10 µg) (OriGene Technologies) were transfected with packaging vector pCL-ECO (3.3 µg) into PlatE cells (Invitrogen, UK) using Lipofectamine 2000 (Invitrogen, UK). After 72 h, 1 ml viral supernatants were collected, filtered through a 0.45 µm filter and mixed with 1 ml of fully supplemented DMEM containing 6 µg/ml PolyBrene (Sigma, UK) and added to MC38 cells (2×10^5). 24 hr post-infection, medium was replenished and stable cells selected in puromycin (10 µg/ml) for a minimum of 14 days.

Cellular Characterisation Assays

Invasion assays were performed as previously described using the CatS inhibitory antibody, Fsn0503 (Fusion Antibodies, UK).[13] Ten representative field of view images were taken from duplicate membranes using the Nikon DXM1200 digital camera (X 20 objective lens). Results were analysed using Lucia GF 4.60 laboratory imaging and data presented as percentage mean number of invaded cells per field of view ± SEM. Live cell proteolysis assays were performed with 1 X 10^5 MC38 Sc and MC38 S4 cells seeded on cover slips coated in DQ-gelatin (Molecular Probes, UK) supplemented Matrigel (BD Biosciences, UK) and were visualized on the Leica TCS SP5 DMI6000 CS

Accepted Article

confocal microscope with Leica LAS AF software.[13] CatS-like activity and pan-MMP activity was determined by fluorimetric assay as previously described using Cbz-Val-Val-Arg-aminomethylcoumarin [20] (Calbiochem, UK) and 520 MMP FRET substrate XIV (AnaSpec, USA), respectively.

In vivo experiments

All mice used in experiments were between 8 – 12 weeks of age with housing and experimentation carried out in accordance with the Animal (Scientific Procedures) Act 1986, the current UKCCCR guidelines and approved by the Queen's University Ethical Review Committee. C57Bl/6 mice were purchased from Charles Rivers Laboratories and also bred in-house. $CatS^{-/-}$ mice were obtained from J. A. Joyce, Memorial Sloan Ketting Cancer Center, New York with permission from H Chapman, UCSF. The mice were subcutaneously injected with 5 x 10^5 MC38 or B16-F10 cells mixed with reduced growth factor Matrigel to a final concentration of 4 mg/ml (BD Biosciences). Tumour volumes were calculated with digital callipers, using the formula, $V = a \times b^2 \times \pi/6$, where a and b represent the longer and shorter diameter of the tumour, respectively. Data was presented as mean tumour burden (mm^3) per group $\pm$ SEM.

Assessment of vessel functionality

Fluorescein-labelled lectin (*Lycopersicon esculentum*) (Sigma, UK) was injected into the tail vein (1 mg/ml, 100 µl/mouse) and allowed to circulate for 5 min prior to heart perfusion with 10% formalin for 5 min. Tumours were excised, embedded in optimal cutting temperature (OCT) compound and

Accepted Article

sectioned at 10 μm thickness before mounting with Vectashield containing DAPI (Vectorlabs, UK). Tumour vessel permeability was assessed via Evan's blue perfusion for 60 min (tail vein injection, 20 mg/ml, 100 μl/mouse), prior to formalin fixation. Evan's blue content of excised, dried tumours was determined after formamide extraction at 620 nm.

Immunohistochemistry of tumour samples and analysis

Tumour sections were formalin fixed, paraffin-embedded and subjected to immuno-staining as previously described.[13] Antibodies and concentrations used were as follows; rat anti-mouse CD34 (1:50) (Abcam), rabbit anti-human Ki67 (1:300) (Abcam), rat anti-mouse CD45 (1:100) (BD Biosciences, UK), rat anti-mouse CD68 (1:50) (Biolegend, UK) and anti-human CatS (1:200) (R&D Systems).

Mean vessel number (MVN) and vessel area was determined by CD34 staining. A minimum of ten random fields of view per tumour were taken under X 20 and X 40 objective lens (Leica DM5500B microscope and AL software). CD34 positive blood vessels and vessel area were calculated and expressed as the MVN ± SEM and mean area (μm^2) ± SEM, respectively. The percentage of Ki67 positive cells was determined by the selection of four random fields of view per tumour, in each group under X 40 objective lens. Both total cell numbers and Ki67 positive cells were determined and the data presented as mean Ki67 positive cells (%) ± SEM.

In Situ Detection of Apoptosis by TUNEL Staining

Accepted Article

Paraffin-embedded tumour sections were stained for apoptotic cells using terminal deoxynucleotidyl transferase-mediated dUDP-nick-end labelling (TUNEL)-based TumorTACS™ In Situ Apoptosis Detection Kit (R&D Systems, UK) as per the manufacturer's instructions. TUNEL staining was assessed by the random selection of five fields of view per tumour, in each group under X 20 objective lens. The number of TUNEL positive cells were counted and presented as total mean TUNEL positive cells per field of view (Mean ± SEM).

Flow cytometry

Tumours were disaggregated and digested in 0.125% trypsin for 20 min at 37 °C, with agitation. DMEM media (2% FCS) was added to the cell suspension and filtered through a nylon mesh (BD Biosciences, UK) to remove debris. The cell suspension was washed, centrifuged at 1000 *g* and resuspended in sterile PBS to a density of 1 X 10^6 cells/ml. To reduce nonspecific binding, cells were blocked on ice for 10 min using Mouse BD Fc block (BD Biosciences, UK). Cells were then stained, in the dark, on ice for 30 min with optimal antibody concentrations, which was determined by titration experiments. Antibodies used included anti-mouse F4/80 conjugated to PE-Cy7 (EBioscience, UK), anti-human CatS (R&D Systems, UK) conjugated with PE-Cy5 lightning link (Biolegend, UK) as per manufacturer's instructions and anti-mouse CD11b conjugated to APC (BD Biosciences, UK). Flow cytometry was performed with a BD FacsAria II with FacsDiva software and data analysis was performed using Flowjo.

Statistical analysis.

Accepted Article

For the analysis of tumour growth, tumour vessel number, tumour vessel area, proliferation rate and apoptosis, the mean and SEM was established from all tumours in each group investigated. The statistical analyses were performed using the Student t-test to obtain the *p* value within each parameter.

Results

CatS is expressed in murine tumour cell lines

In this current investigation, an immuno-competent tumour model was used to study the contribution of CatS from both the tumour and tumour-associated cells, reflecting the distribution of the protease that has been observed clinically.[15-17] MC38 colorectal adenocarcinoma, B16-F10 melanoma and Lewis lung carcinoma (LLC) cell lines were selected (syngeneic with C57Bl/6 backgrounds) and examined to determine the level of CatS expression. RAW 264.7 macrophage-like cells were used as a positive control and CatS mRNA levels were positively detected in all lines by RT-PCR (Figure 1A). Immunofluorescent microscopy was then used to detect the presence of CatS protein in each of the tumour cell lines using RAW 264.7 cells as a positive control. As anticipated, the RAW 264.7 cells revealed the highest levels of CatS staining, whilst in the tumour lines, MC38 cells produced the most intense staining (Figure 1B). Enhancement of the fluorescence signal in the MC38 cells clearly showed punctate vesicular localisation of the protease, consistent with our previous findings in tumour cells[13] (Supplementary Figure S1). Western blotting was also used to analyse the levels of CatS, but this proved inconclusive due to high background levels (data not shown).

Accepted Article

Previously, we have shown that in human tumour lines, secreted CatS can promote invasion, which could be blocked with a CatS specific antibody-based inhibitor, Fsn0503.[13] Here, we were able to confirm that Fsn0503 similarly inhibited MC38 cell invasion in a dose dependent manner ($p = 0.002$ at 500 nM) (Figure 1C). Taken together, these data demonstrate expression of CatS by MC38 cells, which promotes their invasive potential in a manner akin to what we have previously observed in human tumour cell lines.[13]

Gene silencing of CatS in MC38 cells reduces tumour cell invasive potential

The establishment of CatS-depleted MC38 cell lines was undertaken using retroviral shRNA constructs specific for murine CatS in parallel with a scrambled control. The knockdown of CatS was initially analysed by RT-PCR, where CatS-specific shRNA constructs 3 (S3) and 4 (S4) yielded the most efficient knockdown in CatS mRNA levels (Figure 2A). The effect of CatS knockdown clearly reduced the invasive nature of the transduced cells with the most significant reduction observed in the MC38 S4 cells (62%, $p = 0.0001$) (Figure 2B, experiments carried out at least 3 times). This inhibition is more pronounced than in Figure 1C which is as expected as the antibody-based inhibitor used in Figure 1C will only target extracellular CatS as opposed to the shRNA which diminishes total protein. Immunofluorescent staining for CatS protein was also carried out on the transduced lines, where a marked reduction in CatS protein levels was observed in the MC38 S4 cells compared to the control Sc cells (representative images of MC38 Sc versus

Accepted Article

S4 cells shown in Figure 2C). The MC38 S4 cells were also examined for CatS-like activity, revealing a 59% reduction when compared to both the MC38 Sc cells and un-transfected MC38 cells (Figure 2D).

A live-cell proteolysis assay was undertaken to compare the MC38 S4 and Sc cells in the presence of DQ-gelatin, which upon degradation emits a bright green fluorescence. The degradation of this substrate in the pericellular environment was noticeably blunted by depletion of CatS (Figure 2E), which is in agreement with effects we previously observed in human cell lines with Fsn0503.[13] It is possible that the marked difference we observed was due to alterations in secreted MMP activity, such as MMP2 and MMP9, induced by the deletion of CatS. To address this, supernatants from the cell lines were analysed in a fluorimetric activity assay using a pan-MMP internally quenched substrate, but little difference was observed (Supplementary Figure S2). Finally, prior to *in vivo* experimentation, alterations in the proliferation rate of the MC38 S4 cells when compared to the MC38 Sc control cells was also examined with no discernable differences observed (Supplementary Figure S3).

Depletion of host and tumour-derived CatS attenuates tumour development

In order to first evaluate the contribution of CatS from host cell-derived CatS in the syngeneic model, parental MC38 cells were injected into both C57Bl/6 WT and $CatS^{-/-}$ mice. Daily tumour measurements clearly showed that progression of these tumours was significantly attenuated in the $CatS^{-/-}$ mice

Accepted Article

with a 52% reduction (p = 0.023) in tumour burden observed after 16 days when compared to the tumours from the WT mice (Figure 3A). To confirm that these effects were not specific to MC38 cells, a similar study was performed using B16-F10 cells. Again, a significant reduction in tumour growth was apparent in the tumours from the $CatS^{-/-}$ mice with a 55% (p = 0.015) reduction in tumour burden observed after 14 days (Figure 3B).

With the importance of host cell-derived CatS in tumour progression established, the contribution of the protease from the tumour cells was then evaluated. The CatS-depleted MC38 S4 and scrambled control Sc cells were propagated in both $CatS^{-/-}$ and WT mice. In the initial stages of the study, it appeared that the absence of host CatS was the predominant factor in comparison to tumour-derived CatS, given that by day 10, depletion of the tumour-derived protease had no discernable effect (Figure 3C). However, after 15 days it was apparent that depletion of CatS from either the tumour cells or the microenvironment similarly attenuated tumour development (Figure 3C). Nonetheless, the most pronounced effect was observed when CatS was ablated from both tumour and tumour associated cells (65.7% reduction, p = 0.0016).

Tumour vascularisation and tumour vessel functionality is reduced in CatS-depleted tumour microenvironment

Following completion of *in vivo* studies, tumours were initially analysed by general histological analysis, revealing a robust tumour type with clear vascularisation and little evidence of necrosis (representative images shown

Accepted Article

in Supplementary figure S4). To examine the neovascularisation in more detail, immunohistochemical staining for the endothelial marker, CD34, was performed. This clearly distinguished the neovasculature in the tumours, as highlighted with arrows in Figure 4A. Quantitative analysis of CD34-positive mean vessel number (MVN) from the tumour sections revealed that when CatS was deleted from both the tumour and tumour-associated cells, a significant reduction in MVN was observed ($p = 0.0001$) (Figure 4B). The mean vessel area was also measured in these sections showing that CatS depletion from either source resulted in a significant reduction in vessel area. However as before, the most pronounced effects were observed when the protease was removed from all cell types ($p = 0.0001$) (Figure 4C).

Further qualitative evidence that the tumour vasculature was affected by CatS depletion was provided through perfusion of FITC-labelled lectin to identify functional vasculature. This indicated that the vessels appeared more poorly defined in the tumours that lacked CatS from both tumour and tumour-associated cells (Supplementary figure S5). Moreover, the depletion of CatS from either source clearly promoted leakiness of the neovasculature as determined by Evan's blue perfusion, with the most marked effects observed in tumours lacking the protease from both sources ($p = 0.0289$) (Figure 4D). Given the pronounced effects observed on tumour angiogenesis, tumour lysates from the tumour and host CatS positive (WT with Sc cells) versus the tumour and host CatS negative (-/- with the S4 cells) arms were analysed for several angiogenic factors to determine if they were altered by depletion of

Accepted Article

CatS where it was found that both acidic and basic FGF levels were increased (Figure 4E).

CatS depletion results in reduced proliferation and increased apoptosis in tumours

On the basis of the effects observed on tumour neovascularisation, we next examined the tumours for possible alterations in proliferation and apoptosis via Ki67 and TUNEL staining, respectively. The MC38 tumours from all four arms of the investigation stained intensely for Ki67. When CatS was depleted from either the tumour cells or host cells alone, no significant reduction in tumour cell proliferation was apparent (Figure 5A and 5B). However, when CatS was depleted from both sources, a significant reduction in proliferation was clearly observed (17% reduction, $p = 0.0017$) (Figure 5B).

Furthermore, we also examined the tumour sections for apoptosis by TUNEL staining and as highlighted by arrows in Figure 5C, it was found that the decrease in proliferation was complimented by an increase in apoptosis, again most significantly when CatS was depleted from both tumour and tumour associated cells ($p = 0.0012$) (Figure 5D).

Tumour, macrophage and endothelial cells contribute CatS to the tumour microenvironment

Finally, we wished to further clarify the different cellular contributors of CatS to the microenvironment in these MC38 tumours. Immunohistochemical detection of CatS from the tumours using the MC38 Sc line in the WT animals

Accepted Article

clearly showed diffuse positive staining for the protease, which was decreased as expected in tumour sections from each of the CatS-depleted arms, most noticeably in depleted host and tumour (Figure 6A). Upon closer examination of these stained sections, it was revealed that the MC38 Sc tumours in WT mice demonstrated intense CatS positivity in the tumour endothelium compared to the MC38 S4 cells in the $CatS^{-/-}$ mice as highlighted by arrows in Figure 6B i & ii.

Determination of macrophage-derived CatS contribution was undertaken by FACS. Tumours were excised and pooled to generate single cell suspensions and tumour-associated macrophages were selected using F4/80 and CD11b markers and further assessed for CatS positivity. The scatter plot revealed a population of $CD11b^{+}/F4/80^{+}$ cells (4.8%), which demonstrated varying levels of CatS positivity (Figure 6C). A similar finding of macrophages with varying CatS levels has been recently observed in 4T1 tumours using a CatS affinity binding probe.[21]

Discussion

In this current study, we aimed to bridge the gap between clinical observations and prior murine studies, whereby the contribution of CatS from both tumour cells and recruited host cells within the tumour microenvironment was examined. Upon validation of the expression and functionality of CatS in the colorectal carcinoma cell line MC38, we conducted *in vivo* studies with paired scrambled and CatS-depleted MC38 cell lines in wild-type and $CatS^{-/-}$

Accepted Article

animals. We showed that the ablation of CatS had a considerable impact on tumour development and progression; most significantly when CatS was depleted both from tumour (via shRNA knockdown) and tumour-associated cells (via $CatS^{-/-}$ host background). These results mirror the combinative effects of tumour and stroma-derived contribution of cathepsin B which has previously been observed in the MMTV-(PyMT) mammary tumour model.[22]

Cysteine cathepsins have previously been implicated in tumourigenesis, facilitating various tumour-associated processes such as invasion, metastasis and angiogenesis.[8,23] However, amongst these proteases, CatS has unique properties in that it is stable at neutral pH and is a potent elastase and collagenase.[24] Furthermore, it has been suggested to have more physiological importance than other cysteine cathepsins in processing proteins in the extracellular microenvironment.[25] Indeed, given that CatS has been shown to promote the activation of other cysteine cathepsins and normally demonstrates restricted expression largely confined to APCs,[1,25] it may represent a more pertinent therapeutic target than other family members in cancer.

The de-regulated expression of CatS has been identified in a range of human tumour types including lung, brain, colorectal and prostate carcinomas.[11-17, 26] It is known that CatS can be up-regulated by a number of tumour-associated angiogenic factors such as VEGF and bFGF,[20,27] but mechanisms underpinning this remain poorly defined and clearly warrant research in the future.

Accepted Article

Interestingly, recent analysis of over 3100 tumour specimens across 26 cancers, established that chromosome region 1q21.2 where the *CatS* gene is located is frequently somatically amplified. This is a consequence of the addiction of tumours to the anti-apoptotic gene *Mcl-1* found at this locus, and therefore, it is possible that the up-regulation of CatS may be a collateral effect of tumours adopting this anti-apoptotic phenotype.[28]

In this current study, the major effect caused by the stratified deletion of CatS clearly highlighted deficiencies in developing tumour neovasculature. The analyses revealed that loss of CatS reduced the mean vessel number and area and resulted in impaired functionality of the tumour vasculature. These effects are in agreement with previous studies that have highlighted a clear pro-angiogenic role for CatS in tumour development.[10,13,18,19] The impact of impaired tumour vascularization and integrity was complemented with a clear reduction in proliferation and increased apoptosis in these tumours. This is in agreement with the observations of Wang *et al.* using the RIP1-Tag2 model.[18] Interesting, another study using the same RIP1-Tag2 model observed no alterations in proliferation with CatS deletion, which may be attributed to differences in study design or assays employed.[10] Given that no effect was observed on the proliferation rate of the transfected MC38 cells *in vitro*, the noted reduction *in vivo* may be attributed to defective tumour vascularisation. Furthermore, Wang *et al*, reported an increase in tumour FGF concentrations induced by the deletion of CatS, which was similarly observed in our studies. This suggests that the CatS-depleted tumours may have activated alternative pro-angiogenic mechanisms in order to overcome the impediment on

Accepted Article

neovascularization caused by the lack of CatS, which has been observed previously with other anti-angiogenic compounds.[29,30] An additional finding noted in this present model was that vessel leakiness within the tumours was increased in the absence of CatS. This could be a consequence of improper ECM and/or endothelial cell-to-cell junction proteolytic processing, mediated by CatS. This suggests that CatS may have more intricate roles in controlling neoangiogenesis. Indeed, a recent investigation into post-translational modification of endostatin showed that CatS may also have anti-angiogenic roles,[31] highlighting that this protease may indeed mediate both pro- and anti-angiogenic effects to promote coordinated neovascularization.

In addition to the production of CatS by the tumour cells, further analysis of microenvironmental contributors confirmed that TAMs produced the protease as previously shown in the RIP1-Tag2, MMTV-Pymt and 4T1 tumour models.[10,19,21,34] Here, we also found that endothelial cells were CatS positive, confirming CatS up-regulation previously detected at the mRNA level in murine tumour-associated endothelium.[32]

In conclusion, these studies have clearly shown that CatS can be contributed to the tumour microenvironment by both tumour cells and tumour-associated cells in this syngeneic model. These studies also show a mechanism by which tumour-associated cells promote tumour neoangiogenesis and proliferation, and further validates CatS as a therapeutic target. These results are particularly relevant given the recent finding that CatS can be up-regulated[33] by front-line chemotherapies may also contribute to chemotherapy

Accepted Article

resistance.[34] Furthermore, this model provides a useful platform for the evaluation of CatS inhibitors in future studies.

Acknowledgements

This work was supported by the Medical Research Council research grant (G0901615) and by a studentship awarded to D.M.S. from the Department of Education and Learning.

Financial Disclosure

R.E.B, J.A.J and C.J.S. own shares in Fusion Antibodies Ltd.

Accepted Article

Figure legends.

Figure 1. Characterization of CatS expression in syngeneic tumour cell lines. (A) LLC, MC38, B16-F10 tumour cells and RAW 264.7 monocytic cells were analyzed by RT-PCR for CatS at the mRNA level, revealing the presence of mRNA in all cell lines. GAPDH was used as a loading control. (B) Representative images demonstrated CatS expression in these cells lines by the immuno-fluorescent staining of CatS and counterstained with DAPI. X 40 objective lens. Scale bar = 25 μm & 50 μm. (C) Invasion assay performed with Fsn0503 antibody inhibited the invasion of MC38 cells through the matrigel in a modified Boyden chamber invasion assay (38% at 500nM). Isotype control used at 750nM n=3, Error bars, SEM. ** p = 0.002.

Figure 2. Depletion of CatS decreases invasive potential of MC38 cell line. (A) RT-PCR analysis of CatS at the RNA level in MC38 cells upon retroviral transfection and transductions with the murine CatS-specific shRNA constructs and scrambled control shRNA under puromycin selection. The RT-PCR data highlighted substantial knockdown with constructs 3 (S3) and 4 (S4). GAPDH was used as a loading control. (B) Invasion assay demonstrated a reduction in the invasive potential of MC38 cells retrovirally transduced with S3 and S4 constructs when compared to both scrambled control (Sc) and untreated MC38 cells, were a 62% reduction in invasion was noted with the MC38 S4 cells when compared to the MC38 Sc cells. Error bars, SEM. **** p = 0.0001, *** p = 0.0008, n=3. (C) Representative images of the immunofluorescent staining for CatS in the MC38 S4 cells revealed a

Accepted Article

reduced level of expression when compared to the MC38 Sc cells. Cells counterstained with DAPI. X 40 objective lens. (D) Cell lysates (100 µg) were analysed for CatS-like activity and the MC38 S4 cells were found to demonstrate a reduction in CatS-like activity over controls. Error bars (SEM) not visible in MC38 or S4 traces due to minor differences in replicates. (E) Cell-based proteolysis assay with MC38 S4 and Sc cells demonstrated a reduction in pericellular fluorescence in the MC38 S4 cells when compared to MC38 Sc cells. X 40 objective lens. Scale bar = 50 µm.

Figure 3. Ablation of CatS attenuates tumour growth and development *in vivo*. (A & B). MC38 cells (A) and B16-F10 cells (B) were subcutaneously injected into male C57Bl/6 and $CatS^{-/-}$ mice and tumours were measured daily with digital calipers. Data are mean tumour volume (mm^3) ± SEM (n=12 per group) * p = 0.023 for MC38 tumours and * p = 0.015 for B16-F10 tumours. (C) MC38 S4 and Sc cells were subcutaneously injected into both C57Bl/6 (WT) and $CatS^{-/-}$ mice. Tumour measurements were taken as previously indicated. Data are mean tumour volume (mm^3) ± SEM (n=10 per group). Error bars, SEM. * p = 0.016, ** p = 0.001.

Figure 4. Depletion of host and tumour-derived CatS diminishes tumour-associated neovascularisation. (A) Representative images demonstrating the immunohistochemical staining for CD34 to visualize and quantify tumour vasculature within the tumours from each group. Arrows highlight the CD34 positive tumour vessels in each group. X 20 objective lens. Scale bar = 100 µm. (B) Quantitative analysis demonstrated that the loss of functional tumour

Accepted Article

and host CatS from the tumours produced a significant reduction in the mean vessel number (MVN) in the MC38 S4 tumours in the $CatS^{-/-}$ mice when compared to the MC38 Sc tumours in the WT mice. Data shown as MVN from ten tumours in each group, with ten fields of view per tumour assessed. Error bars, SEM. **** p = 0.0001. (C) Mean vessel area was also significantly reduced in all the groups when compared to the MC38 Sc tumours from the WT mice with the most significant effect observed in the MC38 S4 tumours in the $CatS^{-/-}$ mice. Data shown as mean vessel area from ten tumours in each group. Error bars, SEM. * p = 0.0214, *** p = 0.0008, **** p = 0.0001. (D) The depletion of functional tumour and host CatS demonstrated a significant increase in tumour vessel leakiness when compared to MC38 Sc tumours in the WT mice tumours as measured by Evans blue dye perfusion. Data shown as µg Evans blue dye per mg of pooled tumour tissue. Error bars, SEM. * p = 0.0289. n=3. Statistical analysis performed using the Student t-test. (E) MC38 Sc tumours from the WT mice and MC38 S4 tumours from the $CatS^{-/-}$ mice were pooled, lysed and assessed for both acidic and basic fibroblast growth factor (FGF). Almost a 2-fold increase in acidic FGF and 1.5-fold increase in basic FGF was noted in the MC38 S4 tumours from the $CatS^{-/-}$ mice when compared to the MC38 Sc tumours from the WT mice. Error bars, SEM.

Figure 5. Loss of host and tumour-derived CatS decreases tumour proliferation and increases apoptosis (A) Representative images of immunohistochemical staining for tumour cell proliferation using the proliferative marker, Ki67, in each tumour from each group. X 40 objective lens. Scale bar = 100 µm. (B) Quantification of Ki67 positivity revealed

Accepted Article

decrease in proliferation due to the loss of CatS. Typically, four fields of view per tumour were assessed. Data shown as mean Ki67 positive cells (%) assessed from ten tumours in each group. Error bars, SEM. ** p = 0.0017. (C) Representative images of immunohistochemical staining for tumour apoptosis (as highlighted with arrows) using TUNEL staining in each tumour from each group. X 20 objective lens. Scale bar = 100 μm. (D) Quantification of TUNEL staining revealed increase in levels of apoptosis through the loss of CatS. Typically, five fields of view per tumour were assessed. Data shown as mean apoptotic cell number assessed from ten tumours in each group. Error bars, SEM. ** p = 0.0012. Statistical analysis performed using the Student t-test.

Figure 6. Cellular contributors of CatS in the MC38 tumour microenvironment. (A) Representative images of immunohistochemical staining for CatS in the tumours from each group. X 40 objective lens. Scale bar = 100 μm. (B(i) and (ii)) Further immunohistochemical analysis demonstrated that CatS positivity noted in these tumours was also attributed to the endothelium (highlighted by arrows) in the tumour vasculature which was also found to be CatS positive (i) when compared to tumours which lacked CatS (ii). X 40 objective lens. Scale bar = 100 μm. (C) FACS analysis of pooled MC38 Sc tumours from the WT mice revealed that $F4/80^{+}/CD11b^{+}$ population of macrophages. Further characterization of this $F4/80^{+}/CD11b^{+}$ TAM population revealed sub-populations with varying levels of CatS positivity.

References

1. Riese RJ, Mitchell RN, Villadangos JA, Shi GP, Palmer JT, Karp ER,

Accepted Article

De Sanctis GT, Ploegh HL, Chapman HA. Cathepsin S activity regulates antigen presentation and immunity. *J Clin Invest* 1998;**101**:2351-633.

2. Shi GP, Villadangos JA, Dranoff G, Small C, Gu L, Haley KJ, Riese R, Ploegh HL, Chapman HA. Cathepsin S required for normal MHC class II peptide loading and germinal center development. *Immunity* 1999;**10:**197–206.

3. Shi GP, Munger JS, Meara JP, Rich DH, Chapman HA. Molecular cloning and expression of human alveolar macrophage cathepsin S, an elastinolytic cysteine protease. *J Biol Chem* 1992;**267**:7258–7262.

4. Brömme D, Steinert A, Friebe S, Wiederanders B, Kirschke H. The specificity of bovine spleen cathepsin S. A comparison with rat liver cathepsins L and B. *Biochem J* 1989;**264**:475-481.

5. Pozgan U, Caglic D, Rozman B, Nagase H, Turk V, Turk B. Expression and activity profiling of selected cysteine cathepsins and matrix metalloproteinases in synovial fluids from patients with rheumatoid arthritis and osteoarthritis. *Biol Chem* 2010;**391**:571–579.

6. Taleb S, Clément K. Emerging role of cathepsin S in obesity and its associated diseases. *Clin Chem Lab Med* 2007;**45**:328-332.

Accepted Article

7. Lafarge JC, Naour N, Clément K, Guerre-Millo M. Cathepsins and cystatin C in atherosclerosis and obesity. *Biochimie* 2010;**92**:1580-1586.

8. Mohammed MM and Sloane BF. Cysteine Cathepsins: multifunctional enzymes in cancer. *Nat Rev Cancer* 2006;**6**:764-775.

9. Small DM, Burden RE, Scott CJ. The emerging relevance of the cysteine protease Cathepsin S in diseases. *Clin Rev Bon Miner Metab* 2011;**9**:122-132

10. Gocheva V, Zeng W, Ke D, Klimstra D, Reinheckel T, Peters C, Hanahan D, Joyce JA. Distinct roles for cysteine cathepsin genes in multistage tumorigenesis. *Genes Dev* 2006;**20**:543-556.

11. Fernández PL, Farré X, Nadal A, Fernández E, Peiró N, Sloane BF, Shi GP, Chapman HA, Campo E, Cardesa A. Expression of cathepsins B and S in the progression of prostate carcinoma. *Int J Cancer* 2001;**95**:51-55

12. Bunatova K, Obermajer N, Kotyza J, Pesek M, Kos J. Levels of cathepsins S and H in pleural fluids of inflammatory and neoplastic origin. *Int J Biol Markers* 2009;**24**:47-51.

13. Burden RE, Gormley JA, Jaquin TJ, Small DM, Quinn DJ, Hegarty SM,

Accepted Article

Ward C, Walker B, Johnston JA, Olwill SA, Scott CJ. Antibody-Mediated inhibition of Cathepsin S blocks colorectal tumor invasion and angiogenesis. *Clin Cancer Res* 2009;**15**:6042**–**6051.

14. Flannery T, Gibson D, Mirakhur M, McQuaid S, Greenan C, Trimble A, Walker B, McCormick D, Johnston PG. The clinical significance of cathepsin S expression in human astrocytomas. *Am J Pathol* 2003;**163**:175-182.

15. Flannery T, McQuaid S, McGoohan C, McConnell RS, McGregor G, Mirakhur M, Hamilton P, Diamond J, Cran G, Walker B, Scott C, Martin L, *et al.* Cathepsin S expression: An independent prognostic factor in glioblastoma tumours – A pilot study. *Int J Cancer* 2006;**119**:854-860.

16. Flannery T, McConnell RS, McQuaid S, McGregor G, Mirakhur M, Martin L, Scott C, Burden R, Walker B, McGoohan C, Johnston PG. Detection of cathepsin S cysteine protease in human brain tumour microdialysates in vivo. *Br J Neurosurg* 2007;**21**:204–209.

17. Gormley JA, Hegarty SM, O'Grady A, Stevenson MR, Burden RE, Barrett HL, Scott CJ, Johnston JA, Wilson RH, Kay EW, Johnston PG, Olwill SA. The role of Cathepsin S as a marker of prognosis and predictor of chemotherapy benefit in adjuvant CRC: a pilot study. *Br J Cancer* 2011;**105**:1487-1494.

Accepted Article

18. Wang B, Sun J, Kitamoto S, Yang M, Grubb A, Chapman HA, Kalluri R, Shi GP. Cathepsin S controls angiogenesis and tumor growth via matrix-derived angiogenic factors. *J Biol Chem* 2006;**281**:6020-2029.

19. Gocheva V, Wang HW, Gadea BB, Shree T, Hunter KE, Garfall AL, Berman T, Joyce JA. IL-4 induces cathepsin protease activity in tumor associated macrophages to promote cancer growth and invasion. *Genes Dev* 2010;**24**: 241–255.

20. Ward C, Kuehn D, Burden RE, Gormley JA, Jaquin TJ, Gazdoiu M, Small D, Bicknell R, Johnston JA, Scott CJ, Olwill SA. Antibody targeting of cathepsin S inhibits angiogenesis and synergistically enhances anti-VEGF. *PLoS One* 2010;**5**:12543.

21. Verdoes M, Edgington LE, Scheeren FA, Leyva M, Blum G, Weiskopf K, Bachmann MH, Ellman JA, Bogyo M. A nonpeptidic cathepsin s activity-based probe for noninvasive optical imaging of tumor-associated macrophages. *Chem Biol* 2012;**19**:619-28.

22. Vasiljeva O, Papazoglou A, Krüger A, Brodoefel H, Korovin M, Deussing J, Augustin N, Nielsen B.S, Almholt K, Bogyo M, Peters C, and Reinheckel T. Tumor cell–derived and macrophage-derived cathepsin B promotes progression and lung metastasis of mammary cancer. *Cancer Res* 2006;**66**:5242-5250

23. Shi GP, Sukhova GK, Kuzuya M, Ye Q, Du J, Zhang Y, Pan JH, Lu ML,

Accepted Article

Cheng XW, Iguchi A, Perrey S, Lee AM, *et al*. Deficiency of the cysteine protease cathepsin S impairs microvessel growth. *Circ Res* 2003;**92**:493-500.

24. Vasiljeva O, Dolinar M, Pungercar JR, Turk V, Turk B. Recombinant human procathepsin S is capable of autocatalytic processing at neutral pH in the presence of glycosaminoglycans. *FEBS Lett* 2005;**579**:1285-1290.

25. Jordans S, Jenko-Kokalj S, Kühl NM, Tedelind S, Sendt W, Brömme D, Turk D, Brix K. Monitoring compartment-specific substrate cleavage by cathepsins B, K, L, and S at physiological pH and redox conditions. *BMC Biochem*. 2009;**10**:23.

26. Kos J, Sekirnik A, Kopitar G, Cimerman N, Kayser K, Stremmer A, Fiehn W, Werle B. Cathepsin S in tumours, regional lymph nodes and sera of patients with lung cancer: relation to prognosis. *Br J Cancer* 2001;**85**:1193-1200.

27. Liuzzo JP, Petanceska SS, Devi LA. Neurotrophic factors regulate cathepsin S in macrophages and microglia: A role in the degradation of myelin basic protein and amyloid beta peptide. *Mol Med.* 1999;**5**:334-343.

28. Beroukhim R, Mermel CH, Porter D, Wei G, Raychaudhuri S, Donovan

Accepted Article

J, Barretina J, Boehm JS, Dobson J, Urashima M, Mc Henry KT, Pinchback RM, Ligon AH, *et al.* The landscape of somatic copy-number alteration across human cancers. *Nature* 2010;**463**:899-905.

29. Casanovas O, Hicklin DJ, Bergers G, Hanahan D. Drug resistance by evasion of antiangiogenic targeting of VEGF signaling in late-stage pancreatic islet tumors. *Cancer Cell 2005*;**8**:299-309.

30. Carmeliet P, Jain RK. Principles and mechanisms of vessel normalization for cancer and other angiogenic diseases. *Nat Rev Drug Discov* 2011;**10**:417-427.

31. Veillard F, Saidi A, Burden RE, Scott CJ, Gillet L, Lecaille F, Lalmanach G. Cysteine cathepsins S and L modulate anti-angiogenic activities of human endostatin. *J Biol Chem* 2011;**286**:37158-37167.

32. Ryschich E, Lizdenis P, Ittrich C, Benner A, Stahl S, Hamann A, Schmidt J, Knolle P, Arnold B, Hämmerling GJ, Ganss R. Molecular fingerprinting and autocrine growth regulation of endothelial cells in a murine model of hepatocellular carcinoma. *Cancer Res* 2006;**66**:198-211.

33. Burden RE, Gormley JA, Kuehn D, Ward C, Kwok HF, Gazdoiu M, McClurg A, Jaquin TJ, Johnston JA, Scott CJ, Olwill SA. Inhibition of Cathepsin S by Fsn0503 enhances the efficacy of chemotherapy in

Accepted Article

colorectal carcinomas. *Biochimie* 2012;**94**:487-93.

34. Shree T, Olson OC, Elie BT, Kester JC, Garfall AL, Simpson K, Bell-McGuinn KM, Zabor EC, Brogi E, Joyce JA. Macrophages and cathepsin proteases blunt chemotherapeutic response in breast cancer. *Genes Dev* 2011;**25**:2465-2479.

FIGURE 1

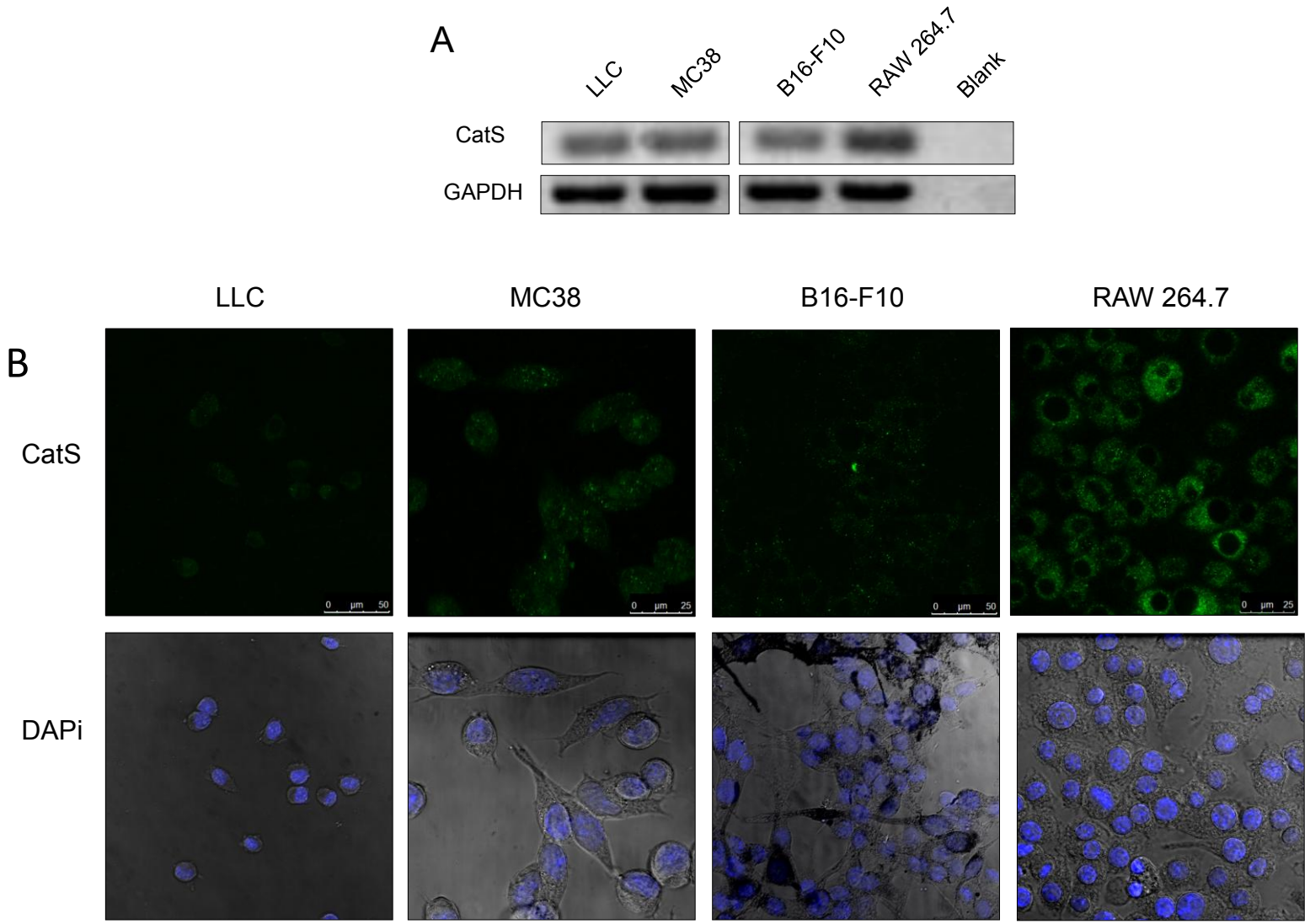
A
LLC
MC38
B16-F10
RAW 264.7
Blank
CatS
GAPDH
LLC
MC38
B16-F10
RAW 264.7
B
CatS
DAPi

C

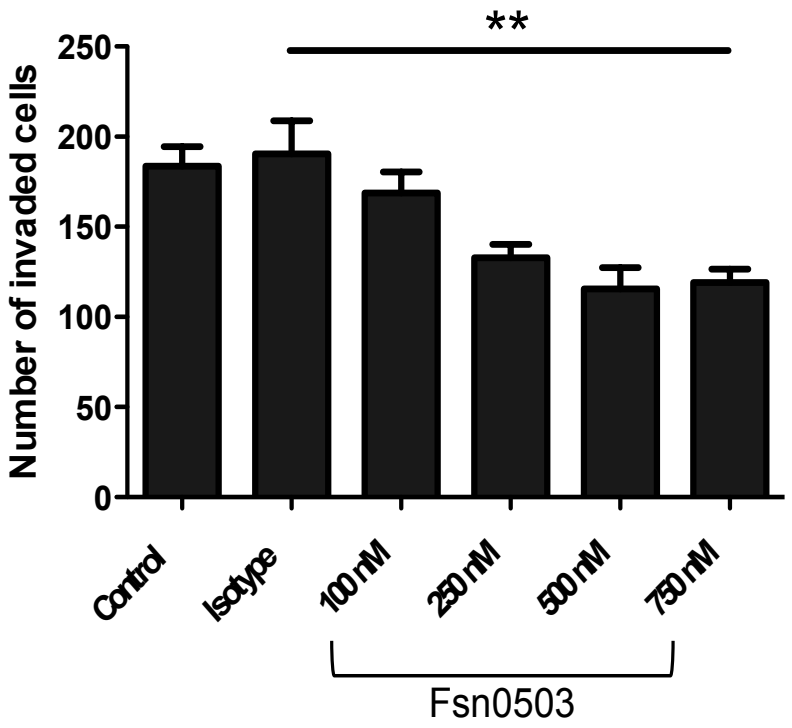
**
Number of invaded cells
250
200
150
100
50
0
Control
Isotype
100 nM
250 nM
500 nM
750 nM
Fsn0503

FIGURE 2

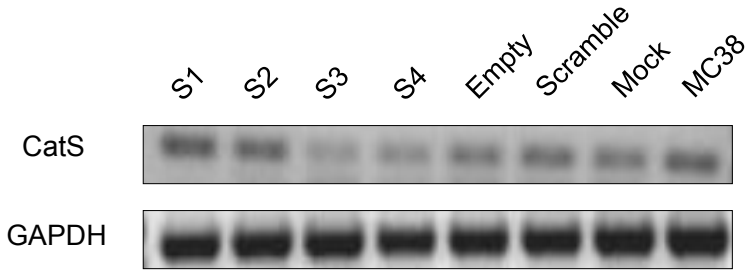

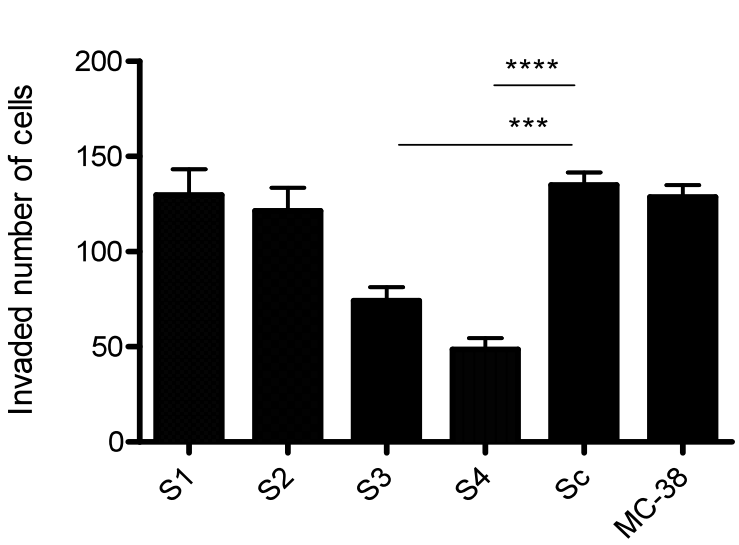

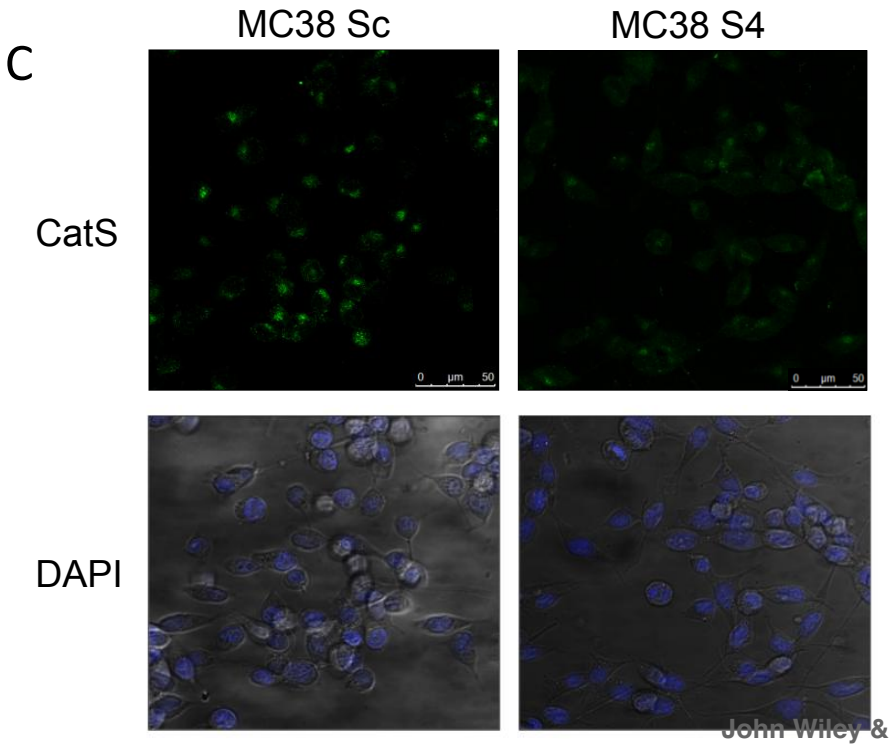

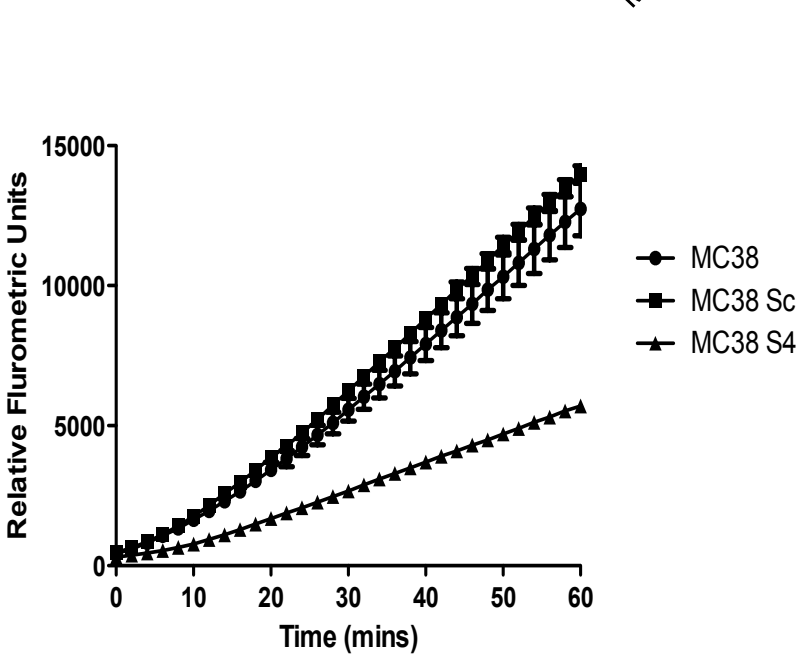

John Wiley & Sons, Inc.

E

MC38 Sc

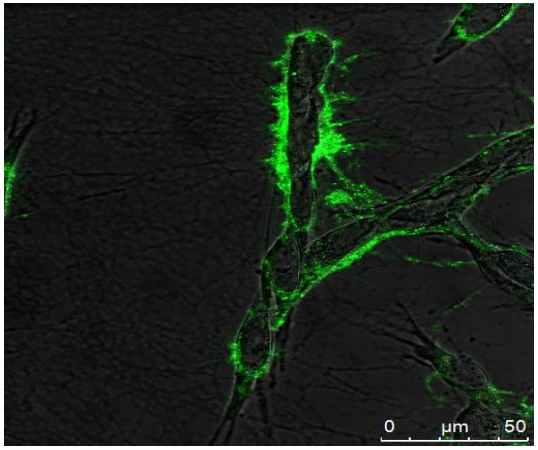

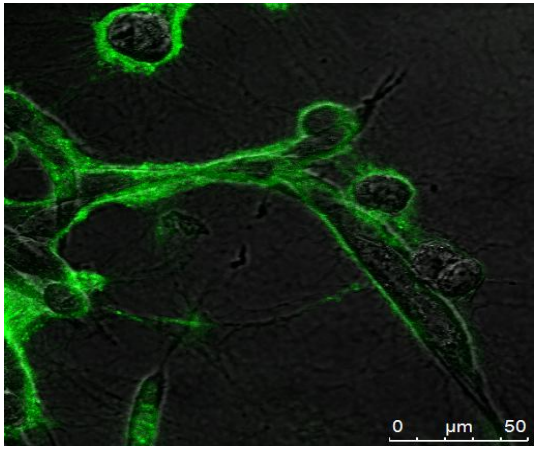

MC38 S4

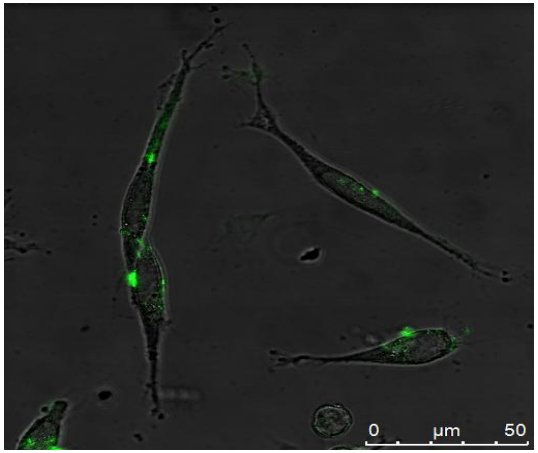

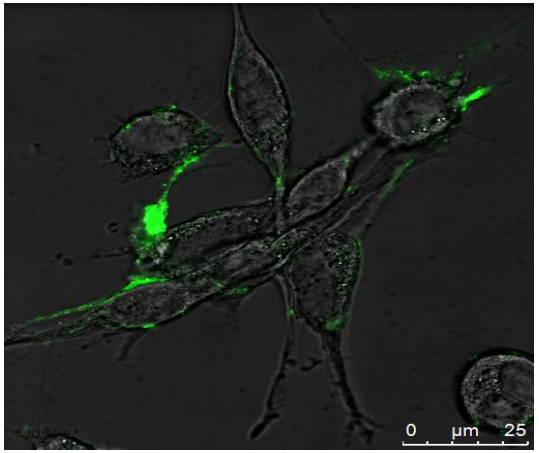

FIGURE 3

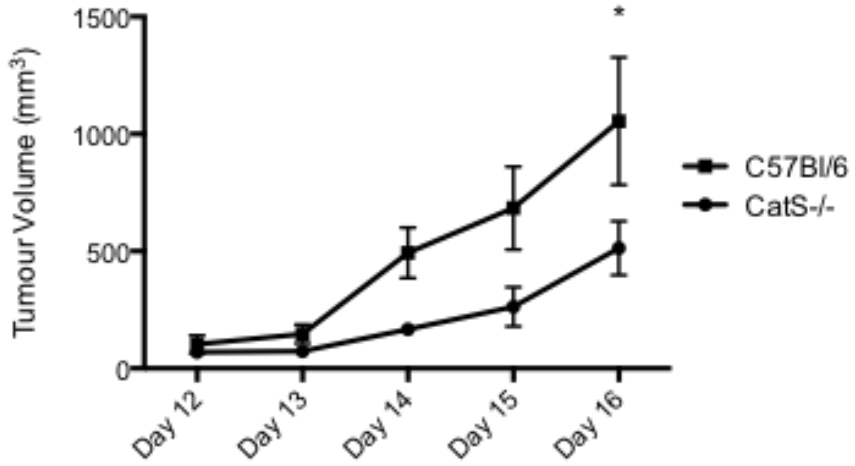

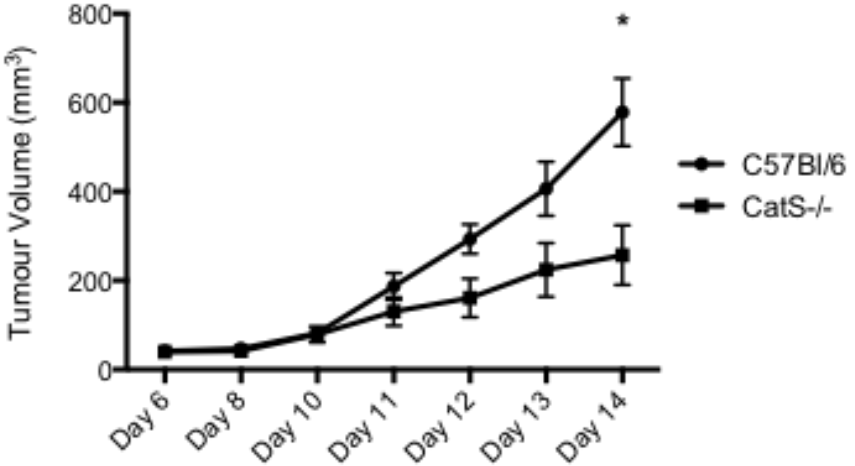

C

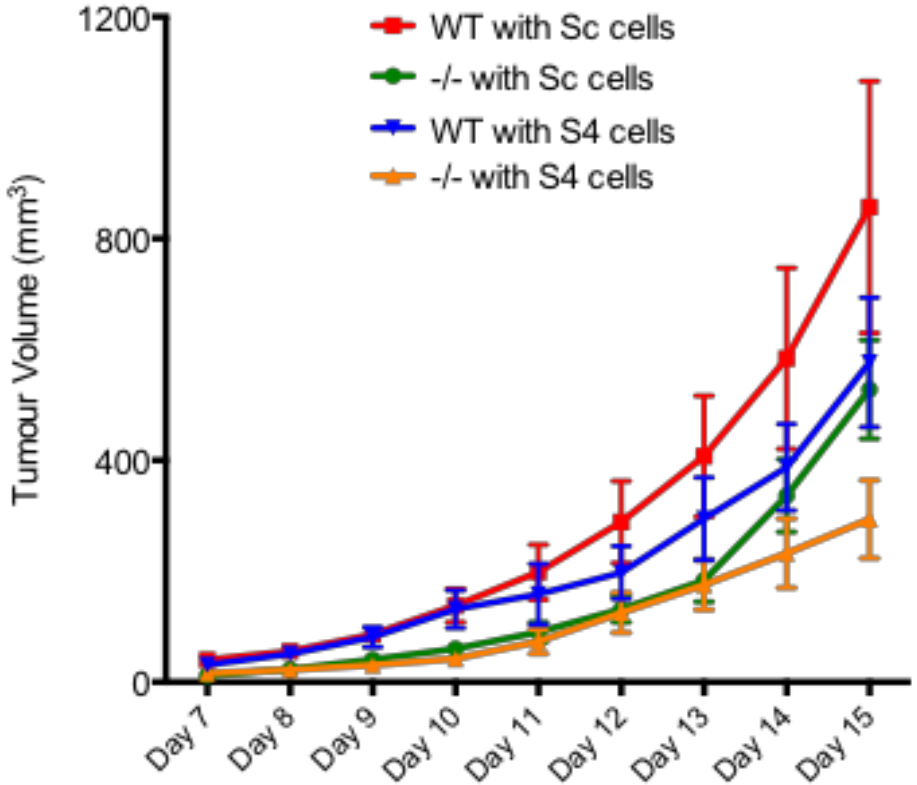

Arm comparisons	% Tumour reduction (*p* value)
WT with Sc versus -/- with Sc	38.4% (*p* = 0.016) *
WT with Sc versus WT with S4	32.7% (*p* = 0.436) ns
WT with Sc versus -/- with S4	65.7% (*p* = 0.001) **
WT with S4 versus -/- with S4	49.1% (*p* = 0.006) **

John Wiley & Sons, Inc.

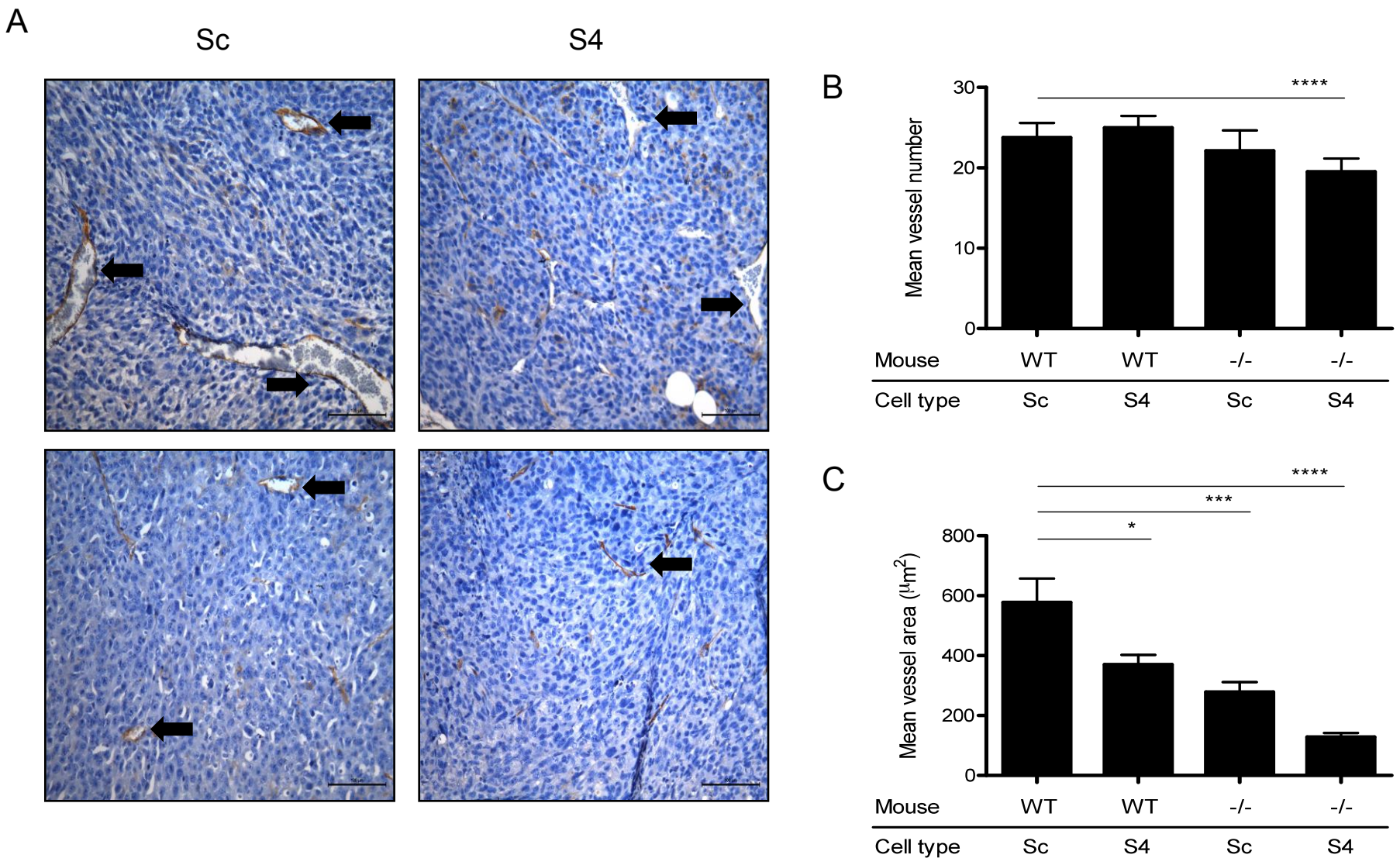
A
Sc
S4
B
Mean vessel number
30
20
10
0
****
Mouse
WT
WT
-/-
-/-
Cell type
Sc
S4
Sc
S4
C
Mean vessel area (μm2)
800
600
400
200
0
****
***
*
Mouse
WT
WT
-/-
-/-
Cell type
Sc
S4
Sc
S4

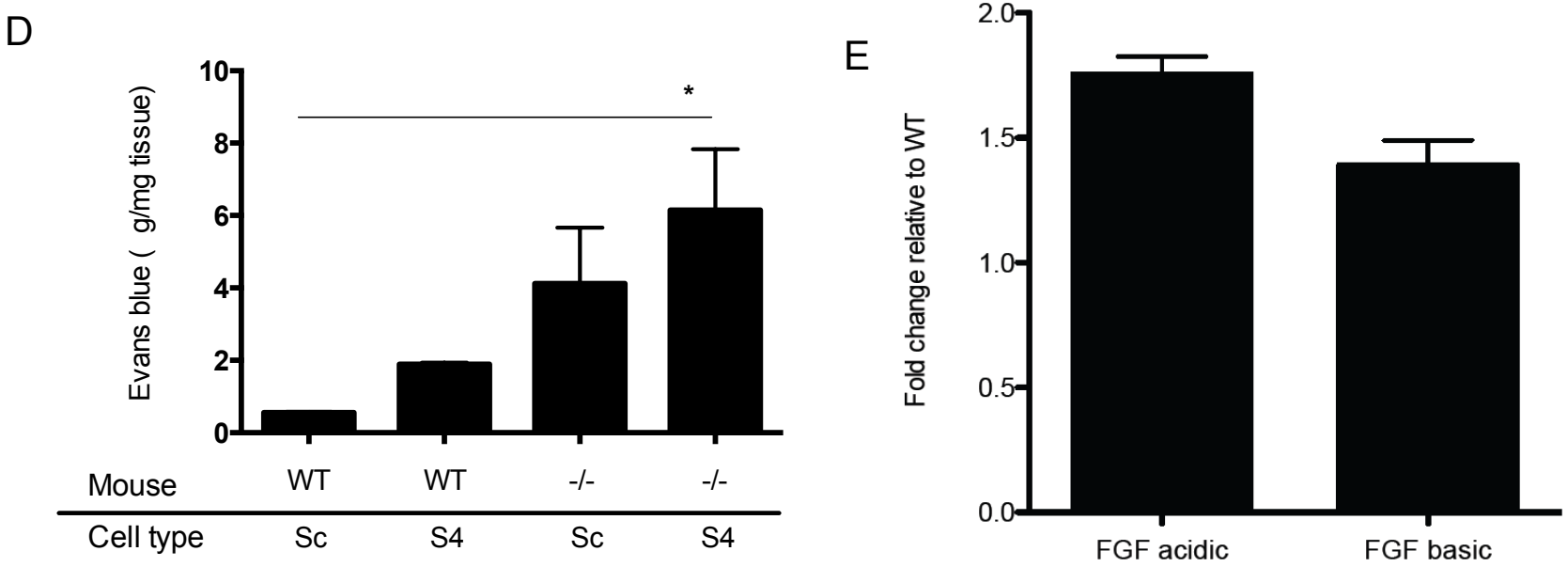
D
Evans blue (g/mg tissue)
10
8
6
4
2
0
*
Mouse
WT
WT
-/-
-/-
Cell type
Sc
S4
Sc
S4
E
Fold change relative to WT
2.0
1.5
1.0
0.5
0.0
FGF acidic
FGF basic

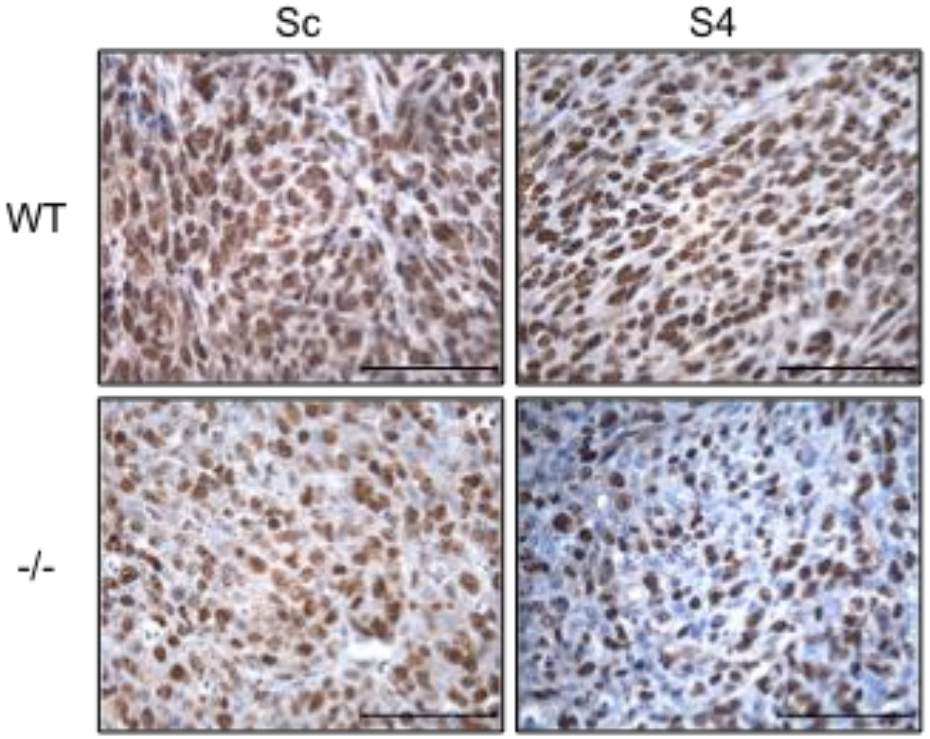

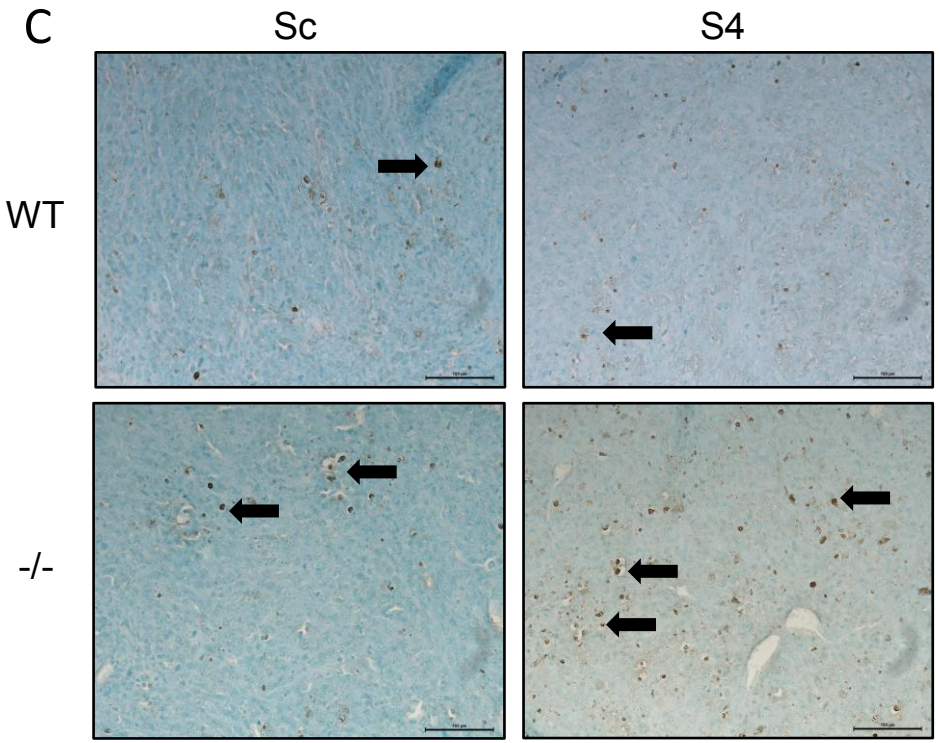

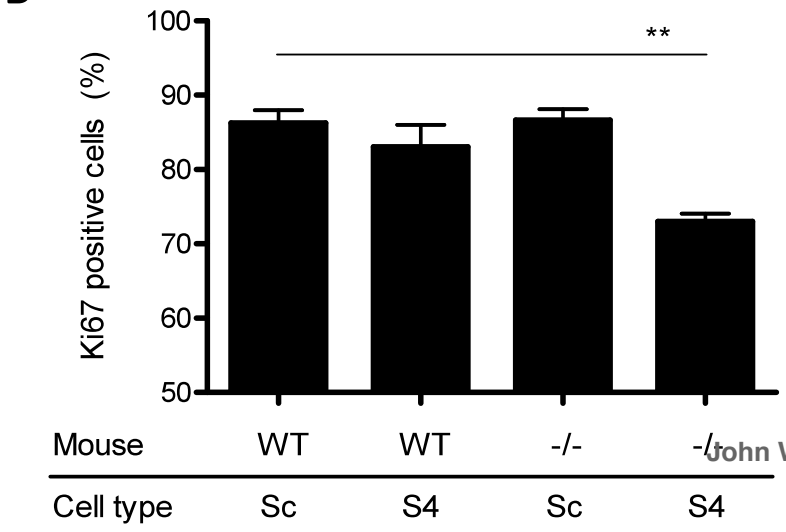

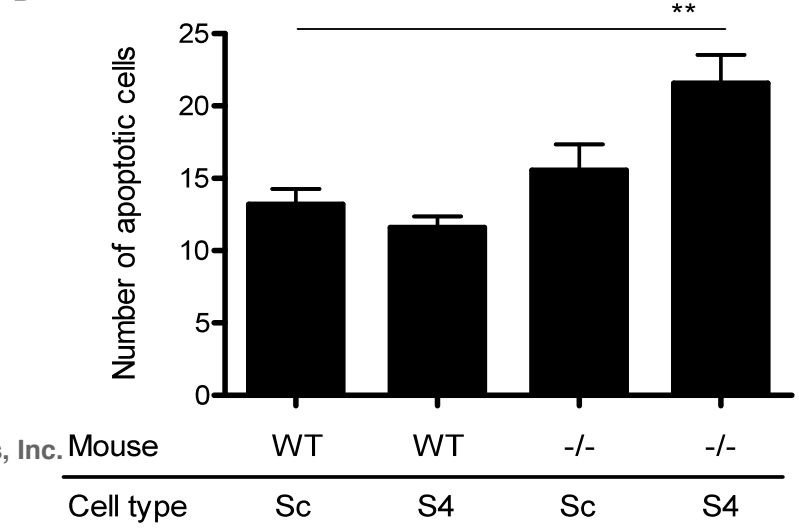

John Wiley & Sons, Inc.

Figure 6

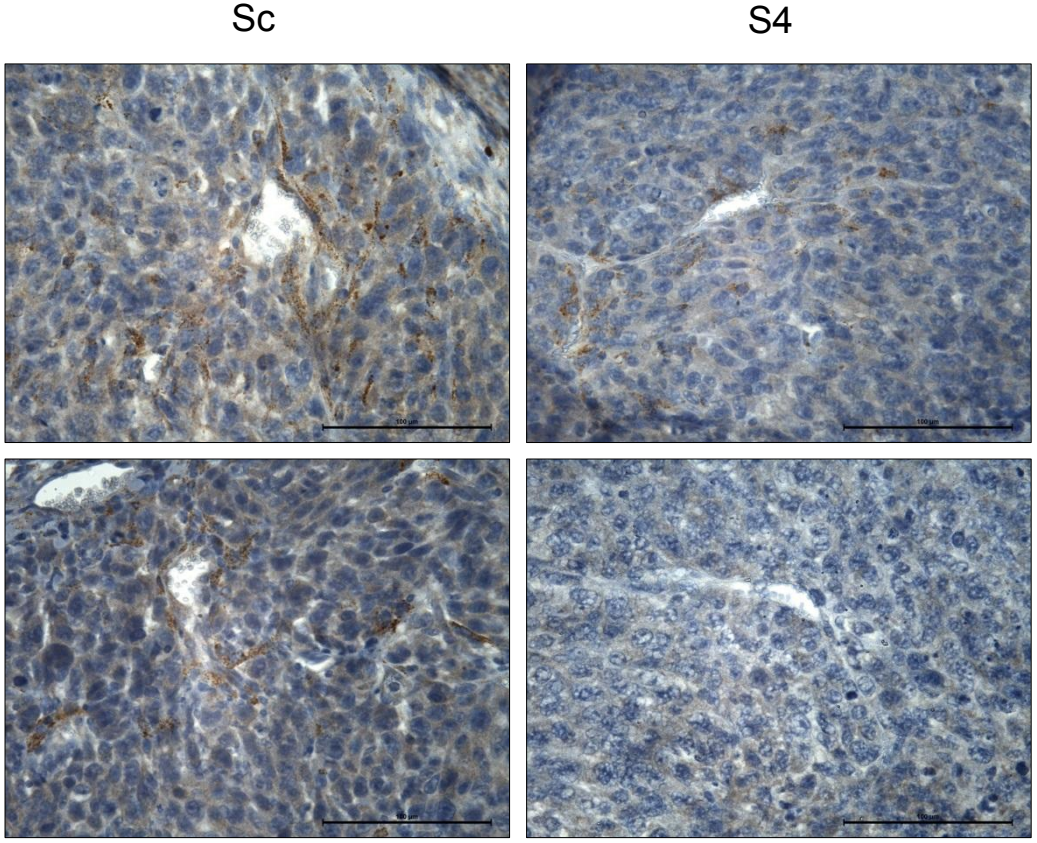

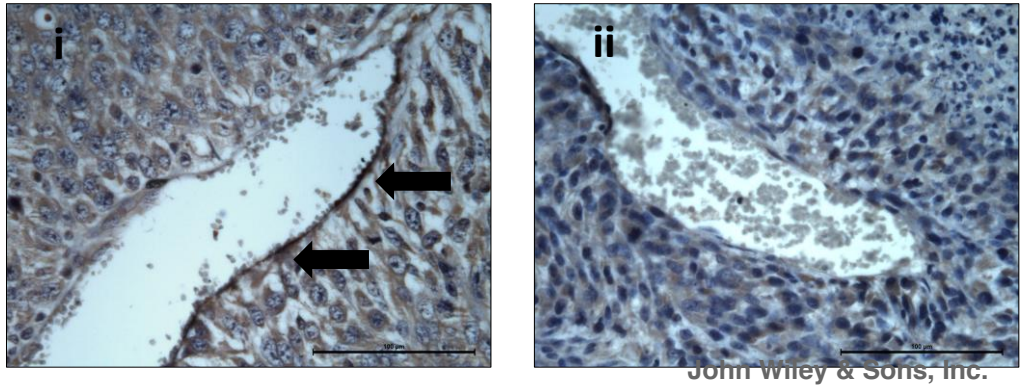

WT with Sc cells

-/- with S4 cells

C

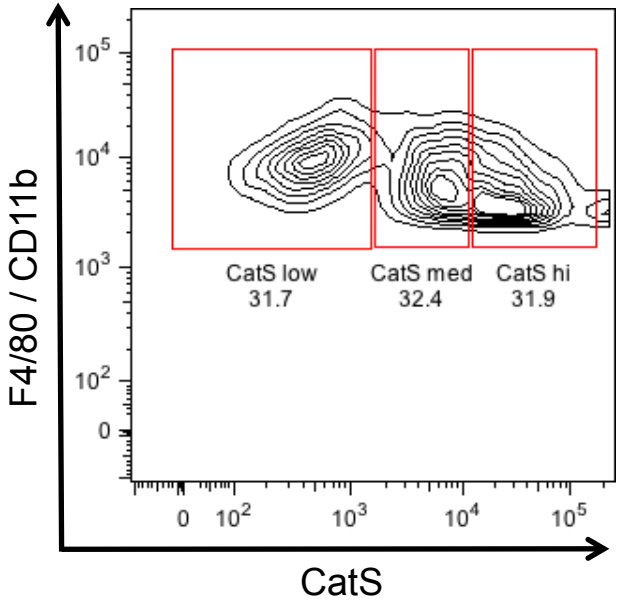

John Wiley & Sons, Inc.

Accepted Article

Supplementary figure S1

Confocal micrograph of MC38 cells showing punctate vesicular staining of CatS. Fluorescence intensity increased after data acquisition using Leica Microsystems LAS AF suite software. X 40 objective lens. Scale bar = 50 μm.

Supplementary figure S2

Tumour cell conditioned media (50 μg) from the MC38 Sc and MC38 S4 cells were analysed for pan-MMP extracellular activity. No apparent alteration in activity between the MC38 S4 cells and control MC38 Sc cells was observed. Assays were repeated in duplicate with the resultant activity displayed as specific activity (RFU min-1 ug-1). Error bars, SEM.

Supplementary figure S3

MC38 S4 and MC38 Sc cells ($1x10^4$) were seeded into 6-well plates and cells counts performed every 24 hrs. It was noted that no difference in the proliferative rate between the two cell types existed at any time point. Error bars, SEM. Data representative of at least three individual experiments.

Supplementary figure S4

Representative images of H&E staining of the tumour sections from each arm of the *in vivo* study. X 20 objective lens. Scale bar = 100 μm.

Supplementary figure S5

Accepted Article

Representative images of the tumour vasculature perfused with FITC-labelled lectin. Tumour sections were counter-stained with DAPI and imaged by confocal microscopy. X 20 objective lens. Scale bar = 50 μm.

Supplementary Figure S1

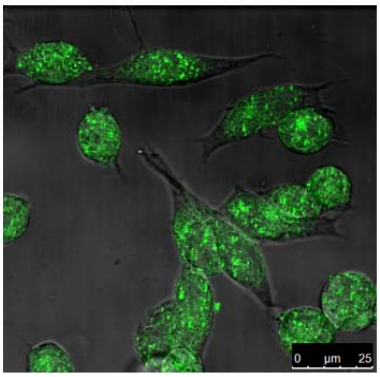

Accepted Article

Supplementary Figure S2

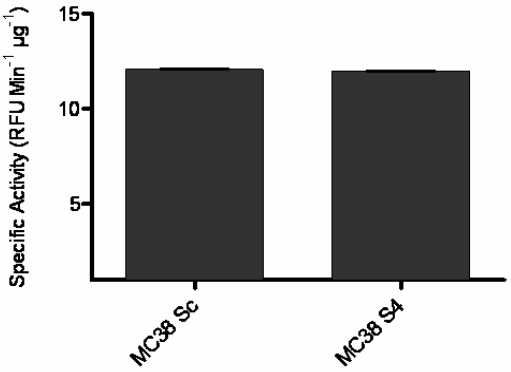

Accepted Article

Supplementary Figure S3

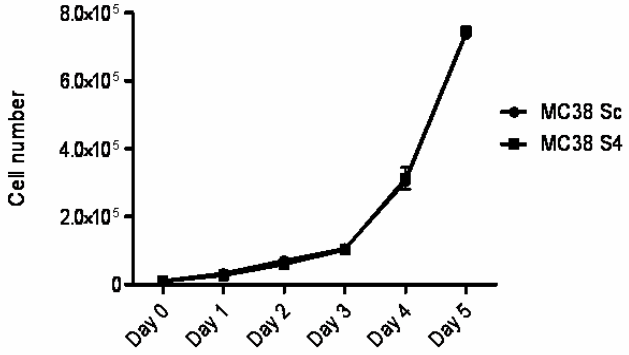

Accepted Article

Supplementary Figure S4

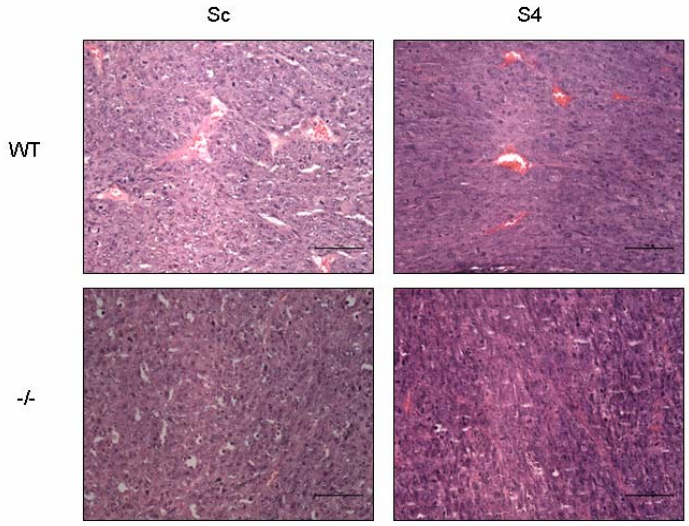

Accepted Article

Supplementary Figure S5